Implementation of MC-SPG Particle Method in the Simulation of Orthogonal Turning Process

P. Rana[1](✉), W. Hintze[2], T. Schall[1], and W. Polley[1]

[1] Mercedes-Benz Group AG, 70546 Stuttgart, Germany
pulkit.rana@mercedes-benz.com
[2] Institute of Production Management and Technology (IPMT), 21071 Hamburg, Germany

Abstract. In the automotive industry, due to fast changing markets and push for implementing novel materials, competitiveness relies increasingly on economical and short planning cycles of machining process. Digitalization has created opportunities for automotive industries to reduce time to market with the help of computer simulations of manufacturing process. In the past decade, particle methods like Smooth Particle Hydrodynamics (SPH), and Smooth Particle Galerkin (SPG), among many others, have been used to simulate machining process. The particle methods have an advantage over classical Finite Element Methods (FEM) as particle methods do not require remeshing or continuous mesh adaptation. Thus, particle methods eliminate the mesh entangling problems in simulation of large plastic deformations, such as machining. This paper describes the application of original SPG and the new Momentum-Consistent-SPG (MC-SPG) method in the orthogonal machining simulation of 1.4837D casted steel material. Furthermore, a study was conducted to understand how different SPG parameters affect simulation results, particularly force components, chip form and temperature. In the end, a Design of Experiment (DoE) was created to study the effects of cutting velocity, feed, and rake angle on force components. The simulation results were experimentally validated, and a good agreement (for cutting forces mean deviation 0–11% and feed forces 4–15%) was found between experimental and simulation results.

Keywords: Machining · Simulation · Finite element method

1 Introduction: Smooth Particle Galerkin Method

Smooth Particle Galerkin (SPG) is a mesh free method developed by Wu et al. [1] for deformation and failure analysis in solid-state mechanics. It is exclusively implemented in Software LS-DYNA. Wu et al. [2] claimed that SPG method can be used for impact and penetration simulations with material failure. This method is based on a mesh-free Galerkin approach to solve the partial differential equations of linear elastic problem. SPG uses a direct node integration method, which, based on the mathematical Eq. (1), can calculate the field variables and their derivatives at the same points [1, 2].

$$M^{\text{lump}} \times \ddot{U} = F_{\text{ext}} - F_{\text{int}} \tag{1}$$

M. Liewald et al. (Eds.): WGP 2022, LNPE, pp. 355–365, 2023.
https://doi.org/10.1007/978-3-031-18318-8_37

Here, M is the lumped mass matrix in diagonal form, $\ddot{U}$ is the vector that contains all particle accelerations. F_{ext} is the external force vector and F_{int} is the regulated internal force term [3].

Solving Eq. (1) can produce spurious-energy modes in the displacement field. To avoid these modes and to reach a stabilization effect, a non-residual stabilization term F_{stab} is added to the SPG formulation. Integration of this stabilization term separately would result in additional computing effort. The new equation system to be solved is shown in Eq. (2) [1, 3].

$$M^{\text{lump}} \times \ddot{U} = F_{\text{ext}} - F_{\text{int}} - F_{\text{stab}} \tag{2}$$

1.1 Momentum-Consistent Smoothed Particle Galerkin

The stabilization in SPG methods is accomplished without the use of a momentum equation residual and therefore they belong to the non-residual stabilization methods. In order to integrate these non-residual stabilization terms, multiple integration points that are matching at each particle are required, which are not computationally efficient. To combat these challenges, a new type of particle stabilization method, called MC-SPG, has been developed. In contrast to most other particle stabilization methods, in MC-SPG, smoothing is not based on residual or non-residual stabilization terms. This does not modify the system of equation and requires only one integration point per particle [4]. A second-order pulse-consistent velocity smoothing algorithm is used in MC-SPG, which is designed to provide accurate and stable results in thermal-structural coupling. The new smoothing algorithm eliminates the stabilization term of the discrete equation and again gives a system of equations the form shown in Eq. (1) [3].

1.2 Application of the SPG Method

Boldyrev et al. [5] simulated the orthogonal cutting of the aluminum alloy (AI6061-T6) using the SPG method. They received qualitative convergence of forces comparable to experimental results. Huang et al. [6] conducted simulations of self-piercing rivet using the SPG method and found a reasonable agreement between experimental and simulation results. Though a comparison between experimental and simulated forces was not performed, a detailed sensitivity analysis was carried out. They found that the choice of critical plastic strain, kernel update interval, dilation parameters, particle spacing, and mass-scaling factor has no significant effect on force results in simulations. Wu et al. [7] applied the SPG method to grinding process simulations and found a good match of reaction forces between simulation and experiment. The comparison of chip shape exhibits that discontinuous chips are formed in both, simulation and experiment. In addition, they found that refinement of the particle distance, kernel update interval and dilation parameters have either insignificant or no influence on force values [7, 8]. Liu et al. [9] implemented the SPG method for removal of blood clots using a high-speed rotating cutting tool. According to authors, a deviation between 3 and 20% was found in simulated cutting force and experimentally determined force. The feed forces were very low in both, simulation, and experiment. Pan et al. [10] implemented SPG modeling

to the simulation of friction drilling process. They found a good match of feed force, torque, and temperature with experiments. In contrast, when using FEM, forecasts were very low. Rana et al. [11] implemented SPG method to orthogonal machining of a casted steel alloy and achieved a good agreement between simulated and experimental force components. For SPG, mean deviations of simulated forces with respect to measured forces amount to 12 and 7% for cutting and feed force respectively. They also compared the simulated chip form with experimentally obtained chip form and found a significant difference between both. However, thermal analysis of orthogonal machining process was not considered here.

This work presents important parameters that need to be used in SPG method for simulating an orthogonal machining process. A coupled thermo-mechanical 3D-orthogonal machining process is simulated, and simulated chip forms and force components are compared to experimental chips and forces.

2 Experimental Setup

The experiments were carried out on a Computerized-Numerical Control lathe Gildemeister CTX310. Hollow cylinders with an outer diameter d = 62 mm, a length l = 40 mm and a wall thickness of t = 1 mm were machined without lubrication under orthogonal conditions with inserts of tungsten carbide HW-K10. The cutting inserts have a clearance angle $\alpha_o = 7°$, rake angle $\Upsilon_o = 0°$ and 15° and cutting edge radii $r_ß$ = 24 μm and 33 μm respectively. The experimental width of cut corresponds to the wall thickness, thus set to $a_p = 1$ mm. A face-centered central composite design was implemented using the Minitab software to evaluate the effect of cutting velocity v_c, feed f and rake angle Υ_o, Table 1. The workpiece material was a casted steel alloy, 1.4837D, containing 11–12% of Nickel [12]. The experimental forces were measured with a 3-component dynamometer Kistler 9121 and were analyzed in DIAdem software. Figure 1 shows force components for $v_c = 180$, $f = 0.25$ and $\Upsilon_o = 0°$. In order to not distort the test results due to existing wear, a different part of cutting edge was used after each cut.

Table 1. Face-centered central composite design

Order	v_c	f	Υ_o	Order	v_c	f	Υ_o
4	180	0.35	0	7	100	0.35	15
8	180	0.35	15	6	180	0.25	15
1	100	0.25	0	5	100	0.25	15
2	180	0.25	0	9	140	0.30	0
10	140	0.30	15	3	100	0.35	0

3 Simulation Setup

The simulations were created in LS-PREPOST, a software from company Ansys. In the simulation model, only the part of the workpiece involved in the machining process is discretized with SPG particles. As SPG particles are computationally expensive, the finite elements were used for the bottom part of the workpiece to reduce the computation time [7]. The workpiece was discretized using hexahedral elements and divided into two parts, which use the same nodes at their point of contact. The division into an SPG and FEM part was achieved by defining different *SECTION keywords. Hence, for the upper part, *SECTION_SOLID_SPG was used which replaced the solid elements with SPG particles. The lower part of the workpiece was defined with keyword *SECTION_SOLID which created finite elements in that part. The cutting inserts were defined as rigid bodies with shell elements, since in this work, no tool wear was taken into account. The workpiece was fixed at bottom in all three directions, while the tool was provided with the cutting velocity. Figure 2 illustrates the discretized model of orthogonal machining in simulations.

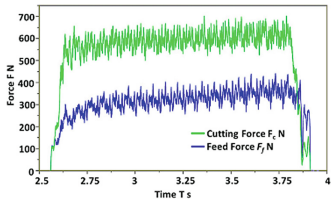

Fig. 1. Force components for $v_c = 180, f = 0.25$ and $\Upsilon_o = 0°$

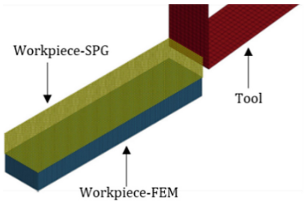

Fig. 2. Discretization of orthogonal cut

To do a coupled 3D-thermo-mechanical analysis, a thermal and mechanical material model for workpiece and tool was defined. Since material properties were assumed to be direction-independent in this work, the keyword *MAT_THERMAL_ISOTROPIC was used. The *MAT_RIGID keyword was used as mechanical material model of the tool because it was modeled as a rigid body. The workpiece uses the Johnson-Cook (JC) material model defined with keyword *MAT_JOHNSON_COOK. This material model is often used for the simulation of machining processes as well as for the simulation of processes with high strain, high strain rates and high temperatures [13, 14]. In LS-DYNA, an equation of state is additionally required to use the JC material model. Hence,

a linear polynomial equation of state was used. The material properties of the workpiece used in simulations are same as mentioned in earlier research work [11].

To control the interaction between workpiece and tool, a contact type must be defined in simulations. For this reason, the keyword *CONTACT_AUTOMATIC_NODES_TO_SURFACE was used [10]. Shear friction model was used in simulations with a coefficient of friction value of 0.5. All simulations were conducted on Dell Precision T7810 tower with Intel(R) Xeon(R) CPU E5-2667 and 32 GB RAM computer.

4 Results and Discussions

In the following section, the effect of various SPG parameters such as ITB, IDAM and ISPLINE on simulation results are analyzed in Sects. 4.1 and 4.2. ITB is a para-meter used to choose the stabilization method, IDAM to choose the failure mechanism and ISPLINE to select the spline function [15]. In the end, the final simulation model results are experimentally validated.

4.1 Parameters Used: ITB = 0, IDAM = 1, ISPLINE = 0

In the first set of simulations, a failure strain (FS) value of 0.25 was used, which was equal to fracture strain. A stretching ratio (STRETCH) of 1.25 was defined. The resulting chip shape is shown in Fig. 3. It was observed that the combination of these parameters do not create chip bending in simulations. However, by assuming unrealistically high values for FS and STRETCH, a chip bend can be achieved. This is also illustrated in Fig. 3 for FS = 500 and STRETCH = 150. These parameters were selected randomly and were only intended to demonstrate the parameters that effect the results drastically. The creation of a chip bend only works reliably for $\Upsilon_o = 15°$. For $\Upsilon_o = 0°$, instead of a chip, a material accumulation is usually created in front of the tool.

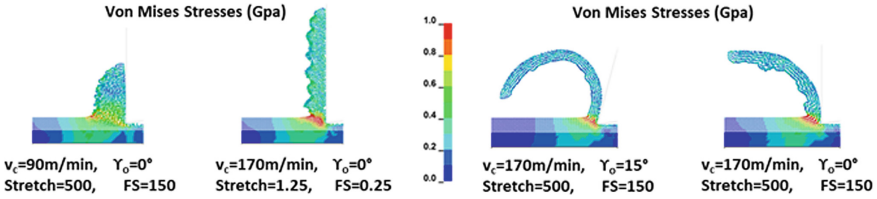

Fig. 3. Influence of the failure parameters on the chip form, $f = 0.2$ mm

4.2 Parameters Used: ITB = 3, IDAM = 13, ISPLINE = 14

For all the simulations mentioned in the previous sections, the parameter IDAM = 1 was used in keyword *SECTION_SOLID_SPG. In the following models, IDAM = 13, which is a modified version of failure mechanism, was defined. According to LS-DYNA, in new mechanism, the bond would break if shear strain is greater than FS, and either tension is higher than STRETCH or Compression is lower than 1/STRETCH.

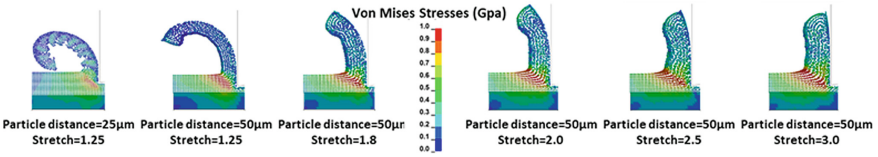

Fig. 4. Influence of STRETCH parameter on chip form

Table 2. Influence of STRETCH parameter on force components

Particle spacing (µm)	STRETCH	Cutting force F_c (N)	Feed force F_f (N)
25	1.25	360	160
50	1.25	410	165
50	1.80	610	250
50	2.00	650	285
50	2.50	720	350
50	3.00	750	355

In previous simulations, a cubic spline function (ISPLINE = 0) was used. It uses brick-shaped nodal support and in case of large body rotation (such as chip bending), the evaluation of the shape function changes with the rotation. To make the range equal to an ellipsoid, ISPLINE = 14 was defined in new simulations. Since the choice of identical dilation parameters creates a sphere in all spatial directions, the chip bending can be observed in simulations. Furthermore, this spline function is intended to better suppress zero-energy modes in pressure-dominant deformations. The comparison of chip form in Fig. 4 shows that the bending of chip decreases with the increase in STRETCH value or particle spacing. In the conducted simulations, a segmented chip was only achieved at the smaller particle spacing of 25 µm. In addition to affecting the chip shape strongly, STRETCH also influences the predicted forces, as shown in Table 2. A higher value of STRETCH increases both, cutting force and feed force. Additionally, cutting force decreases with reduction in particle spacing.

4.3 Final Simulation Models

The final simulation models were built with ITB = 3, IDAM = 13 and ISPLINE = 14. Furthermore, a value of 1.8 was used for all three dilation parameters. Due to the strong dependence of the simulation results on STRETCH value, the dilation parameters were determined empirically. The greatest attention was paid to cutting force, as that was the dominant force compared to other force components. For $\Upsilon_o = 0°$, STRETCH = 2.8 was determined, whereas STRETCH = 2.3 was used for $\Upsilon_o = 15°$. For the tool, a mesh size at the cutting edge rounding was determined by dividing the edge radius by five. A mesh size of 0.1 mm was chosen for the rake and clearance face. A particle spacing of 25 µm was used in the workpiece. It was 12 mm long and 0.05 mm wide, i.e. three

particles were used over the width of the workpiece. The FEM part of the workpiece was 0.425 mm high. The height of SPG part varied with cutting parameters, hence the height of SPG part was 0.25 mm higher than the feed.

5 Comparison of Results

5.1 Force Comparison

To validate a simulation method in machining process, a good approximation of simulated forces with experimental forces is crucial. Both simulations and experiments were carried out according to the test plan mentioned in Table 1. In Fig. 5 (left), the cutting forces of individual experiments are compared to their simulative counterparts. The mean deviation of forces is between 0 and 11%. The deviation of 11% is an exception, which occurs at a rake angle of $\Upsilon_o = 0°$, a cutting velocity of $v_c = 100$ m/min and a feed of $f = 0.35$ mm. A comparison between the feed forces of simulations and experiments is also drawn in Fig. 5 (right). With a deviation of approximately 29%, an exception occurs again for a rake angle of $\Upsilon_o = 0°$, a cutting velocity of $v_c = 100$ m/min and a feed of $f = 0.35$ mm. For the remaining cutting parameters, the feed force deviation is in the range of 4–15%, which indicates a good approximation of the experimental forces in simulations. It is noticeable that the deviation in feed force is always higher for inserts with $\Upsilon_o = 0°$, which could be improved with an increase in STRETCH value.

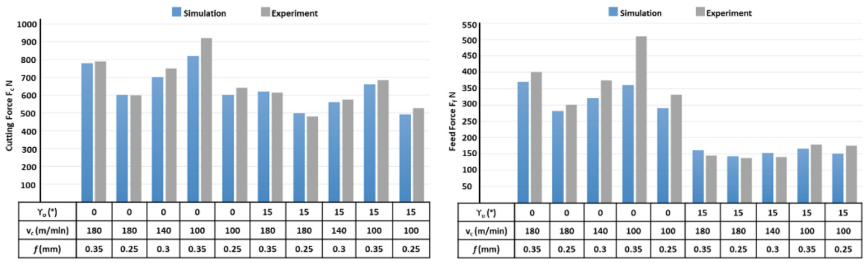

Fig. 5. Comparison of cutting (left) and feed (right) forces between simulations and experiments

Figures 6 and 7 show the influences of rake angle, cutting velocity and feed rate on cutting force and feed force, respectively. These influences are compared for both, experiment and simulation.

As depicted in figures, similar effects can be seen in experiments and simulations, but their characteristics differ. The forces decrease with increase in rake angle and cutting velocity. The significantly high effect of the rake angle is visible in feed force. With the increasing feed, an increase in forces can be observed, as also described by Klocke [16]. A high cutting velocity causes an increase in temperature, which in turn induces thermal softening of material. The softening of material can only be represented to a small extent in simulations and leads to a reduction in forces, which is always higher in experiments than in simulations [16].

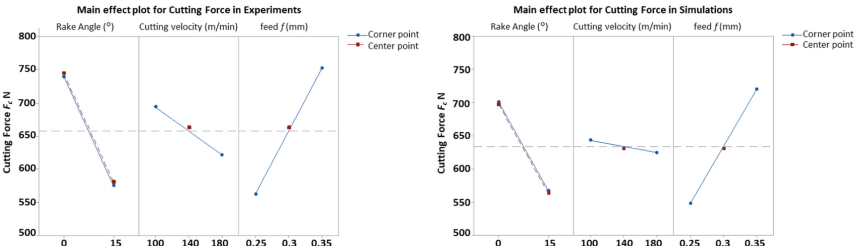

Fig. 6. Main effect diagram for cutting force for experiment and simulation

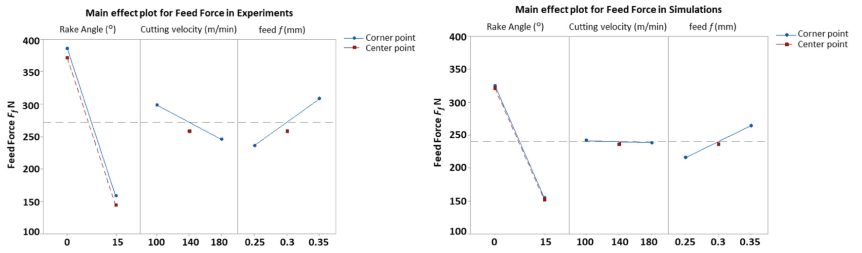

Fig. 7. Main effect diagram for feed force for experiment and simulation

5.2 Comparison of Chip Shape

For an optimal digital replication of machining processes, the simulation should also reliably predict chip formation. However, a comparison of chip shape is very difficult, as it greatly varies within the machining process. Due to this reason, the chips shown below should be seen as a guide, whereby indication of chip thickness is intended to show the scale. A comparison of a simulative and a real chip for rake angle $\Upsilon_o = 0°$ is shown in Fig. 8 (left). A similar curvature with segmented chip can be seen in both simulations and experiments.

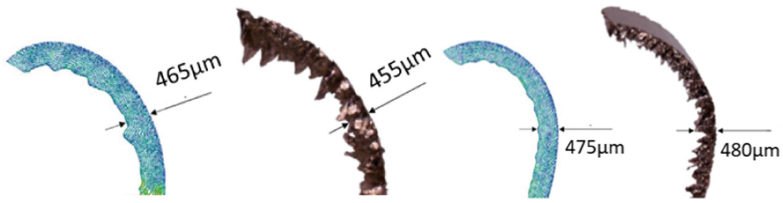

Fig. 8. Chip comparison: simulation versus experiment for $v_c = 100$ m/min, $f = 0.25$ mm and $\Upsilon_o = 0°$ (left) and for $v_c = 180$ m/min, $f = 0.25$ mm and $\Upsilon_o = 15°$ (right)

Figure 8 (right) compares the simulative and experimentally produced chips for cutting edge with a rake angle $\Upsilon_o = 15°$. Here, too, the chip form is comparable to the experimental chip form. However, the segmented chip is not formed in simulations. This can be improved by using a finer distance between the particles at the expense of simulation time.

5.3 Comparison of Chip Temperature

The simulated chip temperatures were not compared to the real temperatures, as they are very difficult to measure. Owing to this reason, it is only checked whether the temperature effects to be expected in reality also occur in simulation. Rana et al. [17] measured temperatures for same material and similar process parameters in a turning process, which were in the same range as simulated temperatures in this work. A comparison of the simulated temperatures for $\Upsilon_o = 0°$ is shown in Fig. 9. To visually illustrate the differences, a maximum value of 650 °C is defined for the temperature scale. Like in real case scenario, the highest temperatures occur on the contact surface between chip and rake face. It can also be seen that the temperature rises with an increase in cutting velocity as well as feed.

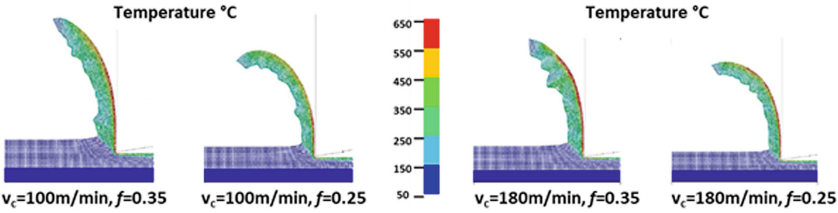

Fig. 9. Comparison of temperature for rake angle $\Upsilon_o = 0°$

In Fig. 10, analogous to Fig. 9, the temperatures occurring in simulations with a rake angle $\Upsilon_o = 15°$ are illustrated. The comparison between the two insert geometries shows that the chip temperature is higher for $\Upsilon_o = 0°$ than for $\Upsilon_o = 15°$. This result meets the expectation that the parameters feed, cutting speed and rake angle while increasing the cutting power lead to higher chip temperatures. Further validation of the simulated temperatures needs to be done by chip temperature measurements.

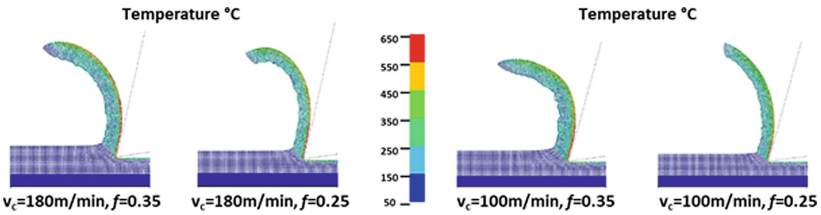

Fig. 10. Comparison of temperature for rake angle $\Upsilon_o = 15°$

6 Conclusion

A thermo-mechanical model of orthogonal machining with the SPG and MC-SPG method for the material 1.4837D was built. Simulation results were validated against

the experimental tests results. It was found that bending of the chip, with the original formulation of the SPG method, can only be achieved by assuming unrealistic values for the parameters controlling the bond breakage. Moreover, the simulated forces had a higher deviation from the experimentally measured forces. Adding to that, no realistic temperature distribution could be simulated. The problem of unrealistic temperature forecasting could be avoided by using the MC-SPG method. The comparison between final simulation models, with MC-SPG formulation, and experiments showed a good approximation of the force values. Furthermore, main effects of individual parameters on the forces of simulation and experiment were in good agreement. Additionally, the simulation predicted the effects of individual cutting parameters on expected temperature according to the relevant literature. The simulated chips represented a realistic form similar to experimental chip forms. However, the simulations could not predict segmented chips accurately for every cutting parameter, but this can be improved by using a finer particle spacing. The validation proves the applicability of the MC-SPG method for simulation of orthogonal machining.

Acknowledgements. The authors would like to thank Mr. Eckhard Zoch for helping in conducting the experiments, Mr. Pitt Held for helping in simulations and LS-DYNA Support Team for its dedicated technical support.

References

1. Wu, C.T., Guo, Y., Hu, W.: An introduction to the LS-DYNA smoothed particle Galerkin method for severe deformation and failure analyses in solids. In: 13th International LS-DYNA Users Conference (2014)
2. Wu, C.T.: Smoothed particle Galerkin formulation for simulating physical behaviors in solids mechanics, US 2015/0112653 A (2014)
3. Wu, C.T., Wu, Y., Lyu, D., Pan, X., Hu, W.: The momentum-consistent smoothed particle Galerkin (MC-SPG) method for simulating the extreme thread forming in the flow drill screwdriving process. Comput. Part. Mechan. **7**(2), 177–191 (2019). https://doi.org/10.1007/s40571-019-00235-2
4. Pan, X., Wu, C.T., Hu, W., Wu, Y.C.: Smoothed particle Galerkin method with a momentum-consistent smoothing algorithm for coupled thermal-structural analysis. In: 15th International LS-DYNA Users Conference (2018)
5. Boldyrev, I.S.: SPG simulation of free orthogonal cutting for cutting forces prediction. In: Radionov, A., Kravchenko, O., Guzeev, V., Rozhdestvenskiy, Y. (eds) Proceedings of the 4th International Conference on Industrial Engineering (2019)
6. Huang, L., Wu, Y., Huff, G., Huang, S., Ilinich, A., Freis, A., Luckey, G.: Simulation of self-piercing rivet insertion using smoothed particle Galerkin method. In: 15th International LS-DYNA Users Conference (2018)
7. Wu, C.T., et al.: Numerical and experimental validation of a particle Galerkin method for metal grinding simulation. Comput. Mech. **61**(3), 365–383 (2017). https://doi.org/10.1007/s00466-017-1456-6
8. Wu, Y., Wu, C.T., Hu, W.: Parametric and convergence studies of the smoothed particle Galerkin (SPG) Method in semi-brittle and ductile material failure analyses. In: 15th International LS-DYNA Users Conference (2018)

9. Liu, Y., Zheng, Y., Li, A.D., Liu, Y., Savastano, L.E., Shih, A.J.: Cutting of blood clots—experiment and smooth particle Galerkin modelling. CIRP Ann. **68**(1), 97–100, ISSN 0007-8506 (2019)
10. Pan, X., Wu, C.T., Hu, W.: A momentum-consistent stabilization algorithm for Lagrangian particle methods in the thermo-mechanical friction drilling analysis. **64**, 625–644 (2019)
11. Rana, P., Zielasko, W., Schuster, T., Hintze, W.: Orthogonal turning simulations for casted steel alloy using mesh free methods. In: Wulfsberg, J.P., Hintze, W., Behrens, B.A. (eds) Production at the Leading Edge of Technology. Springer Vieweg, Berlin, Heidelberg (2019)
12. Kaiser, T.: Entwicklung eines Nickel-reduzierten Austenits als Werkstoff im thermisch hoch beanspruchten Abgasturbolader. Dissertation Universität Clausthal, Universitätsbibliothek, Clausthal-Zellerfeld, Clausthal (2014)
13. Olleak, A.A, El-Hofy, H.A.: Prediction of cutting forces in high speed machining of Ti6Al4V using SPH method. In: Proceedings of the ASME 2015 International Manufacturing Science and Engineering Conference, vol. 1, Charlotte, North Carolina, USA. V001T02A018. ASME (2015)
14. Lampropoulos, A.D., Markopoulos, A.P., Manolakos, D.E.: Modeling of Ti6Al4V alloy orthogonal cutting with smooth particle hydrodynamics: a parametric analysis on formulation and particle density. Metals **9**, 388 (2019)
15. LS-DYNA. Keyword user's manual. vol. I. pp. 3240–3241 (2020)
16. Klocke, F.: Fertigungsverfahren 1—Zerspanung mit geometrisch bestimmter Schneide, vol. 9. Auflage, Springer Vieweg, Aachen (2018)
17. Rana, P., Hintze, W., Schall, T., Polley, W.: Study on the influence of the coating thickness in turning of a hard to machine material using FEM-simulation. In: Behrens, B.A., Brosius, A., Drossel, W.G., Hintze, W., Ihlenfeldt, S., Nyhuis, P. (eds) Production at the Leading Edge of Technology. WGP 2021. Lecture Notes in Production Engineering. Springer, Cham (2022)